Pramana – J. Phys. (2018) 90:16
https://doi.org/10.1007/s12043-017-1508-7

Half-metallic ferromagnetism in Ti_2IrZ (Z = B, Al, Ga, and In) Heusler alloys: A density functional study

K H SADEGHI and F AHMADIAN*

Department of Physics, Shahreza Branch, Islamic Azad University, Shahreza, Iran
*Corresponding author. E-mail: farzad.ahmadian@gmail.com, ahmadian@iaush.ac.ir

MS received 24 June 2017; revised 30 August 2017; accepted 7 September 2017; published online 3 January 2018

Abstract. The first-principle density functional theory (DFT) calculations were employed to investigate the electronic structures, magnetic properties and half-metallicity of Ti_2IrZ (Z = B, Al, Ga, and In) Heusler alloys with $AlCu_2Mn$- and $CuHg_2Ti$-type structures within local density approximation and generalised gradient approximation for the exchange correlation potential. It was found that $CuHg_2Ti$-type structure in ferromagnetic state was energetically more favourable than $AlCu_2Mn$-type structure in all compounds except Ti_2IrB which was stable in $AlCu_2Mn$-type structure in non-magnetic state. Ti_2IrZ (Z = B, Al, Ga, and In) alloys in $CuHg_2Ti$-type structure were half-metallic ferromagnets at their equilibrium lattice constants. Half-metallic band gaps were respectively equal to 0.87, 0.79, 0.75, and 0.73 eV for Ti_2IrB, Ti_2IrAl, Ti_2IrGa, and Ti_2IrIn. The origin of half-metallicity was discussed for Ti_2IrGa using the energy band structure. The total magnetic moments of Ti_2IrZ (Z = B, Al, Ga, and In) compounds in $CuHg_2Ti$-type structure were obtained as $2\mu_B$ per formula unit, which were in agreement with Slater–Pauling rule ($M_{tot} = Z_{tot} - 18$). All the four compounds were half-metals in a wide range of lattice constants indicating that they may be suitable and promising materials for future spintronic applications.

Keywords. Half-metals; Heusler alloys; *ab-initio* calculations; electronic structure; magnetic properties.

PACS Nos **71.15.Mb; 71.20.Lp; 71.20.–b; 75.50.–y**

1. Introduction

Half-metallic (HM) ferromagnets, which exhibit metallic character for one spin state and a semiconducting behaviour for another spin state, have 100% spin-polarisation at the Fermi level. These materials have attracted great attentions due to their potential applications in spintronic devices, such as magnetic sensors, tunnel junctions, and giant magnetoresistance (GMR) [1,2]. De Groot *et al* [3] first explored HM characteristic of the NiMnSb alloy in half-Heusler structure. Until now, HM ferromagnets have been widely found in perovskite compounds, e.g. $BaCrO_3$ [4] and Sr_2FeMoO_6 [5], Heusler alloys, e.g. Co_2MnSi [6] and Mn_2ZnCa [7], metallic oxides, e.g. CrO_2 [8] and Fe_3O_4 [9], dilute magnetic semiconductors (DMSs), e.g. Mn-doped GaN [10] and Cr-doped CdTe [11], and zincblende (ZB) transition-metal pnictides and chalcogenides [12–17]. Among HM ferromagnets, Heusler alloys are attractive because of their technical applications (in spin-injection devices [18], spin-filters [19], tunnel junctions [20], or GMR devices [21,22]), their relatively high Curie temperature compared to other compounds, and their crystal structure similar to conventional semiconductors (zinc-blende and rock-salt types) [23–25]. In order to stabilise Heusler alloys practically, they should be grown on suitable substrates. Because Heusler alloys consist of 4 fcc sublattice, conventional semiconductors with zinc-blende structure (including 2 fcc sublattice) can be used as the substrate. The mismatch between thin film (Hesuler alloys) and the substrate (semiconductors) should be as small as possible to keep the HM character of Heusler alloys in the growth process. Therefore, lattice constant of semiconductors should be chosen close to that of Heusler alloys.

Heusler compounds generally take a cubic crystal structure with a 2:1:1 stoichiometry (X_2YZ) in which X and Y mainly are transition metals and Z is a main group element. X_2YZ Heusler compounds can be characterised with two different types: (1) the cubic $L2_1$ structure with a space group $Fm\bar{3}m$ with prototype of $AlCu_2Mn$ in which X, Y, and Z atoms are placed on the Wyckoff positions 8*c* (1/4, 1/4, 1/4), 4*a* (0, 0, 0), and 4*b* (1/2, 1/2, 1/2), respectively, (2) the $CuHg_2$

Ti-type structure with a space group $F\bar{4}3m$ in which X atoms occupy the nonequivalent 4*a* (0, 0, 0) and 4*c* (1/4, 1/4, 1/4) positions, while Y and Z atoms are located at 4*b* (1/2, 1/2, 1/2) and 4d (3/4, 3/4, 3/4) positions, respectively [26]. In this structure, X atoms are denoted as X(1) and X(2).

The studies on Heusler alloys are mainly relative to Co-based alloys with $L2_1$ structure [27–32]. Furthermore, half-metallicity was recently verified in new Heusler alloys such as Mn_2CoZ (Z=Al, Ga, Si, Ge, Sn, and Sb) [33], Fe_2YSi (Y=Mn and Cr) [34], Cr_2MnZ (Z=P, As, Sb, Bi, and Al) [35,36], V_2YSb (Y=Cr, Mn, Fe, and Co) [37], and Ti_2YZ (Y=Fe, Co, and Ni; Z=Al, Ga, and In) [38], Sc_2CrZ (Z=C, Si, Ge, and Sn) compounds [39], and Pt_2MnGa [40]. There are several studies on Ti-based Heusler alloys such as Ti_2VZ (Z=Al, Ga, In) [41], Ti_2CrSn [42], Ti_2CrSi [43], Ti_2NiB [44], Ti_2MnZ (Z=Al, Si, Ga, Ge, In, Sn, Sb, Bi) [45,46], Ti_2FeZ (Z=Al, Si, Ga, Ge, In, Sn) [47–51], and Ti_2CoZ (Z=B, Al, Si, Ga, Ge, In, Sn) [52–59] in which the Y atom is a 3*d* transition metal element. Recently, Taskin *et al* [60] have investigated the electronic and magnetic properties of the Ti_2RuSn Heusler compound in which Y atom was replaced by Ru (4*d* transition metal element). We decided to replace Y atom with a 5*d* transition metal in Heusler alloys. Therefore, in this paper, the electronic structure and magnetism of Ti_2IrZ (Z = B, Al, Ga, and In) compounds in both $AlCu_2Mn$- and $CuHg_2Ti$-type structures were investigated using first-principle calculations. To date, there is no experimental or theoretical study on Ti_2IrZ (Z = B, Al, Ga, and In) Heusler compounds.

2. Computational method

The calculations were performed using the full-potential linearised augmented plane-wave (FP-LAPW) method within density functional theory (DFT) as implemented in the Wien2k package [61]. The exchange correlation potential (V_{XC}) within the local density approximation (LDA) is calculated using the scheme of Ceperley–Alder as parametrised by Perdew–Zunger [62] and within the generalised gradient approximation (GGA) using the scheme of Perdew–Burke–Ernzerhof (PBE-GGA) [63]. In this method, the crystal is divided into non-overlapping muffin-tin (MT) spheres surrounding the atomic sites and the interstitial regions among MT spheres. The wave functions are expanded terms of spherical harmonic functions inside MT spheres and in Fourier series in the interstitial region. The MT sphere radius for all atoms was chosen as 2 a.u. The potential function and charge density inside the MT spheres were expanded up to $l_{max} = 10$ and the largest vector in Fourier expansion of the charge density was $G_{max} = 12\,(\text{a.u.})^{-1}$. The maximum value of the reciprocal lattice vector in the plane-wave expansion in the interstitial region (K_{max}) was determined to be equal to $8/R_{MT}$, where R_{MT} is the smallest MT sphere radius. The separation energy of the valence and the core electrons was chosen as −6 Ry. A mesh of 84 special *k*-points was made in the irreducible wedge of the Brillouin zone. Self-consistency was achieved by setting the convergence of the charge smaller than 10^{-5} e/a.u.^{3}

3. Results and discussion

3.1 *Structural properties*

First, the structural optimisation was performed by minimising the total energy of Ti_2IrZ (Z = B, Al, Ga, and In) alloys with respect to the variation of unit cell volume for $AlCu_2Mn$- and $CuHg_2Ti$-type structures in ferromagnetic (FM) and non-magnetic (NM) states. Then, the obtained total energies as functions of unit cell volume were fitted to the Murnaghan equation of state [64]. For instance, the obtained energy–volume curves using GGA are shown in figure 1. Accordingly, in all compounds, $CuHg_2Ti$-type structure in FM state is the most stable structure except Ti_2IrB in which $AlCu_2Mn$-type structure is energetically more stable than the other structure. The energy–volume curves of the four compounds in $AlCu_2Mn$-type structure for FM and NM states completely coincide with each other indicating their NM character. The site preference of X and Y atoms is strongly influenced by the number of their valence electrons [26]. When the atomic number of Y is more than that of the X element in Heusler compounds, the compounds crystallise in the $CuHg_2Ti$-type structure. As the valence electrons of Ir are more than those of Ti, it is expected that Ti_2IrZ alloys crystallise in $CuHg_2Ti$-type structure. According to figure 1, three alloys of Ti_2IrZ (Z = Al, Ga, and In) obey this rule, but Ti_2IrB does not show this conventional trend and is considered as an exception. The equilibrium structural parameters including the lattice parameter, bulk modulus, and its derivative are listed in table 1 for Ti_2IrZ (Z = B, Al, Ga, and In) compounds using LDA and GGA. As can be seen, with increasing atomic number of Z atom, the lattice parameters for both structures increase along B→Al sequence, are approximately constant along Al→Ga, and increase along Ga→In, again. There is no experimental or theoretical data to compare with the obtained results. It is obvious that GGA results in higher values with respect to LDA for the lattice parameters. As expected, the GGA underestimates the value of the bulk

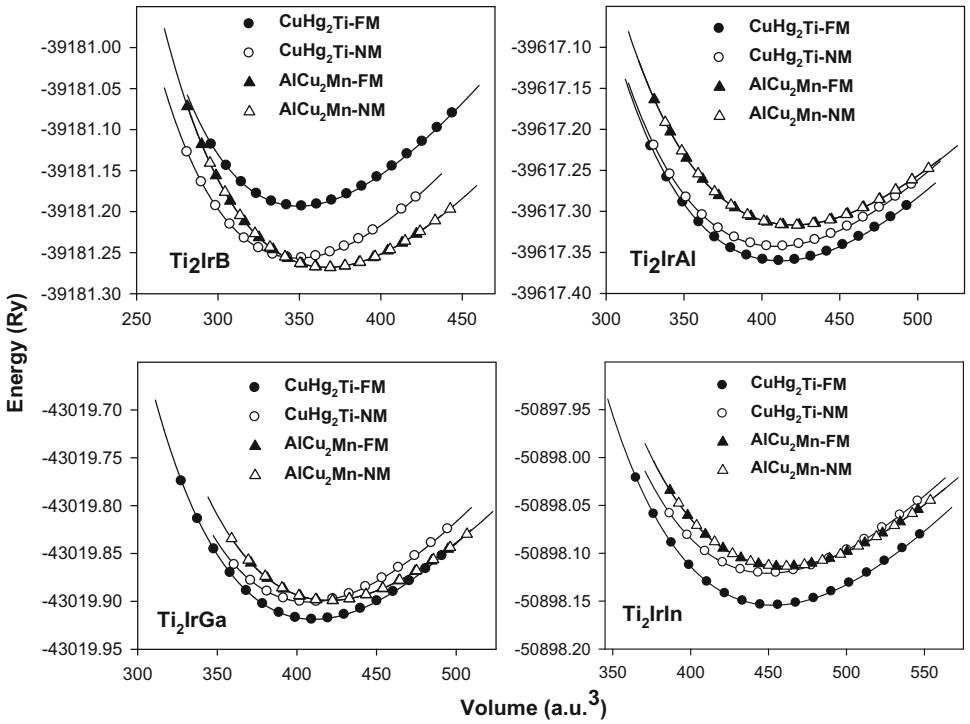

Figure 1. Total energy as a function of unit cell volume for the Ti_2IrZ (Z = B, Al, Ga, and In) compounds for $AlCu_2Mn$-type and $CuHg_2Ti$-type structures in the ferromagnetic (FM) and non-magnetic (NM) states.

modulus in comparison with the LDA. Afterwards, the results are mainly presented with GGA.

The cohesive energy (E_C) measures the strength of the force that binds atoms together in the solid state and is correlated to the structural stability in the ground state. The E_C is presented as

$$E_C^{Ti_2IrZ} = E_{tot}^{Ti_2IrZ} - (2E_{Ti} + E_{Ir} + E_Z), \quad Z = B, Al, Ga, \text{and } In, \tag{1}$$

where $E_{tot}^{Ti_2IrZ}$ is the equilibrium total energy of Ti_2IrZ compounds and E_{Ti}, E_{Ir}, and E_Z are the total energies of isolated atoms. In order to calculate the energy of isolated atoms, each atom is considered in a fcc lattice with a lattice constant of 20 a.u. to ensure that every atom locates on an isolated position. The value of E_C for each structure (table 1) confirms the structural stability of Ti_2IrZ Heusler compounds in $CuHg_2Ti$-type structure except for Ti_2IrB.

Afterward, in order to verify whether Ti_2IrZ Heusler compounds can be fabricated experimentally, the formation energies (E_f) of all alloys are calculated as

$$E_f^{Ti_2IrZ} = E_{tot}^{Ti_2IrZ} - \left(2E_{Ti}^{bulk} + E_{Ir}^{bulk} + E_Z^{bulk}\right), \quad Z = B, Al, Ga, \text{and } In, \tag{2}$$

where $E_{tot}^{Ti_2IrZ}$ is the equilibrium total energy of Ti_2IrZ compounds, and E_{Ti}^{bulk}, E_{Ir}^{bulk}, and E_Z^{bulk} are the total energies of Ti, Ir, and Z elements in the bulk state. The negative formation energies (table 1) show that these four alloys are easily synthesised experimentally and they may be fabricated in laboratory conditions.

3.2 *Electronic properties*

The electronic structure of Ti_2IrZ (Z = B, Al, Ga, and In) Heusler compounds were studied at the equilibrium lattice constant. In the first step, the electronic band structure was calculated to understand the nature of the materials. Figure 2 shows the spin-projected band structures of Ti_2IrGa Heusler compound as a representative of all compounds in both $AlCu_2Mn$- and $CuHg_2Ti$-type structures for majority (spin-up) and minority (spin-down) states. Accordingly, the band structures in $AlCu_2Mn$-type structure are completely similar in majority and minority spin states and the Fermi level intersect the energy bands. Therefore, this compound is called a NM metal with $AlCu_2Mn$-type structure. It is observed that in the $CuHg_2Ti$-type structure, the Fermi level crosses energy bands in majority spin state, while in minority spin state the Fermi level is located within a band gap, indicating the HM characteristic of Ti_2IrGa at the equilibrium lattice constant. Similarly, the other three compounds are NM metals and HM ferromagnets in $AlCu_2Mn$-type and $CuHg_2Ti$-type structures, respectively.

Table 1. The calculated bulk parameters of Ti_2IrZ (Z = B, Al, Ga, and In) compounds in $AlCu_2Mn$-type and $CuHg_2Ti$-type structures for FM and NM states using LDA and GGA. a (Å): lattice parameter, B (GPa): bulk module, B': derivative of bulk module, E_c (Ry): cohesive energy, and E_f (Ry): formation energy.

Compound	Structure	State V_{XC}	a (Å)	B (GPa)	B'	E_c (Ry)	E_f (Ry)
Ti_2IrB	$AlCu_2Mn$	FM-GGA	6.02	183.56	3.83	−1.90	−0.15
		NM-GGA	6.02	182.16	4.00	−1.90	−0.15
		FM-LDA	5.90	190.23	4.10	−1.85	−0.13
		NM-LDA	5.88	194.45	4.34	−1.85	−0.13
	$CuHg_2Ti$	FM-GGA	5.93	197.19	4.33	−1.79	−0.08
		NM-GGA	5.92	196.39	4.17	−1.85	−0.14
		FM-LDA	5.81	203.56	4.65	−1.75	−0.06
		NM-LDA	5.80	202.25	4.47	−1.80	−0.11
Ti_2IrAl	$AlCu_2Mn$	FM-GGA	6.30	155.79	3.99	−1.75	−0.15
		NM-GGA	6.30	155.34	4.09	−1.75	−0.15
		FM-LDA	6.18	167.45	4.27	−1.67	−0.13
		NM-LDA	6.18	166.98	4.48	−1.67	−0.13
	$CuHg_2Ti$	FM-GGA	6.26	165.23	4.14	−1.79	−0.12
		NM-GGA	6.25	164.92	4.20	−1.78	−0.18
		FM-LDA	6.07	177.67	4.35	−1.70	−0.09
		NM-LDA	6.03	175.54	4.51	−1.68	−0.08
Ti_2IrGa	$AlCu_2Mn$	FM-GGA	6.30	159.32	4.42	−1.67	−0.18
		NM-GGA	6.30	158.46	4.37	−1.67	−0.18
		FM-LDA	6.22	167.34	4.69	−1.60	−0.16
		NM-LDA	6.23	165.89	4.60	−1.60	−0.16
	$CuHg_2Ti$	FM-GGA	6.25	167.05	4.32	−1.69	−0.19
		NM-GGA	6.24	169.57	4.68	−1.68	−0.18
		FM-LDA	6.03	175.15	4.60	−1.60	−0.17
		NM-LDA	6.01	177.57	4.91	−1.60	−0.16
Ti_2IrIn	$AlCu_2Mn$	FM-GGA	6.49	145.95	4.54	−1.60	−0.03
		NM-GGA	6.49	146.05	4.51	−1.60	−0.03
		FM-LDA	6.26	155.78	4.80	−1.57	−0.01
		NM-LDA	6.26	158.23	4.78	−1.57	−0.01
	$CuHg_2Ti$	FM-GGA	6.46	152.98	4.44	−1.64	−0.14
		NM-GGA	6.45	153.71	4.70	−1.61	−0.11
		FM-LDA	6.29	165.34	4.70	−1.59	−0.10
		NM-LDA	6.28	167.86	4.93	−1.55	−0.07

In order to analyse the characteristic of the energy bands around the Fermi level, the band structure of Ti_2IrGa in the $CuHg_2Ti$-type structure was investigated in details. The low-lying energy region −10 eV to −7 eV are occupied by Ga s states. The three bands between −6 and −3.5 eV are mainly relative to Ga p states which are hybridised with the d bands of the transition metals located above −3 eV. The Z elements have an important role on the formation of minority band gap. By the hybridisation of the Z elements with transition metals, the Z p shell is filled and the remaining d electrons take part in the $d-d$ hybridisation between transition metals which affects the width of the minority band gap. In fact, Z elements indirectly affect the width of the minority band gap by their different configurations of valence electrons.

In the following, the $d-d$ hybridisation between transition metals, which has a direct role on the formation of minority band gap, is investigated. According to the results reported by Skaftouros *et al* [65], in the case of Heusler compounds with $CuHg_2Ti$-type structure, e.g. Ti_2IrGa Heusler compound, similar symmetry of Ti(1) and Ir atoms causes that their d-orbitals hybridise together creating five bonding d ($2\times e_g$ and $3\times t_{2g}$) and five non-bonding ($2\times e_u$ and $3\times t_u$) states. Then, the five Ti(1)–Ir bonding d states hybridise with the d-orbitals of the Ti(2) atoms and create bonding ($2\times e_g$ and $3\times t_{2g}$) and antibonding states ($2\times e_g^*$ and $3\times t_{2g}^*$). A schematic representation of the $d-d$ hybridisation of Ti_2IrGa compound in the $CuHg_2Ti$-type structure is shown in figure 3. It is clear from figure 2 that for Ti_2IrGa, the five energy bands below the Fermi level in spin minority state from −3.5 to 0 eV are mainly relative to bonding states. The five bands above the Fermi level between 0 and 2.5 eV belong to non-bonding states ($2\times e_u$ and $3\times t_u$), and the five bands between about 2.5 eV

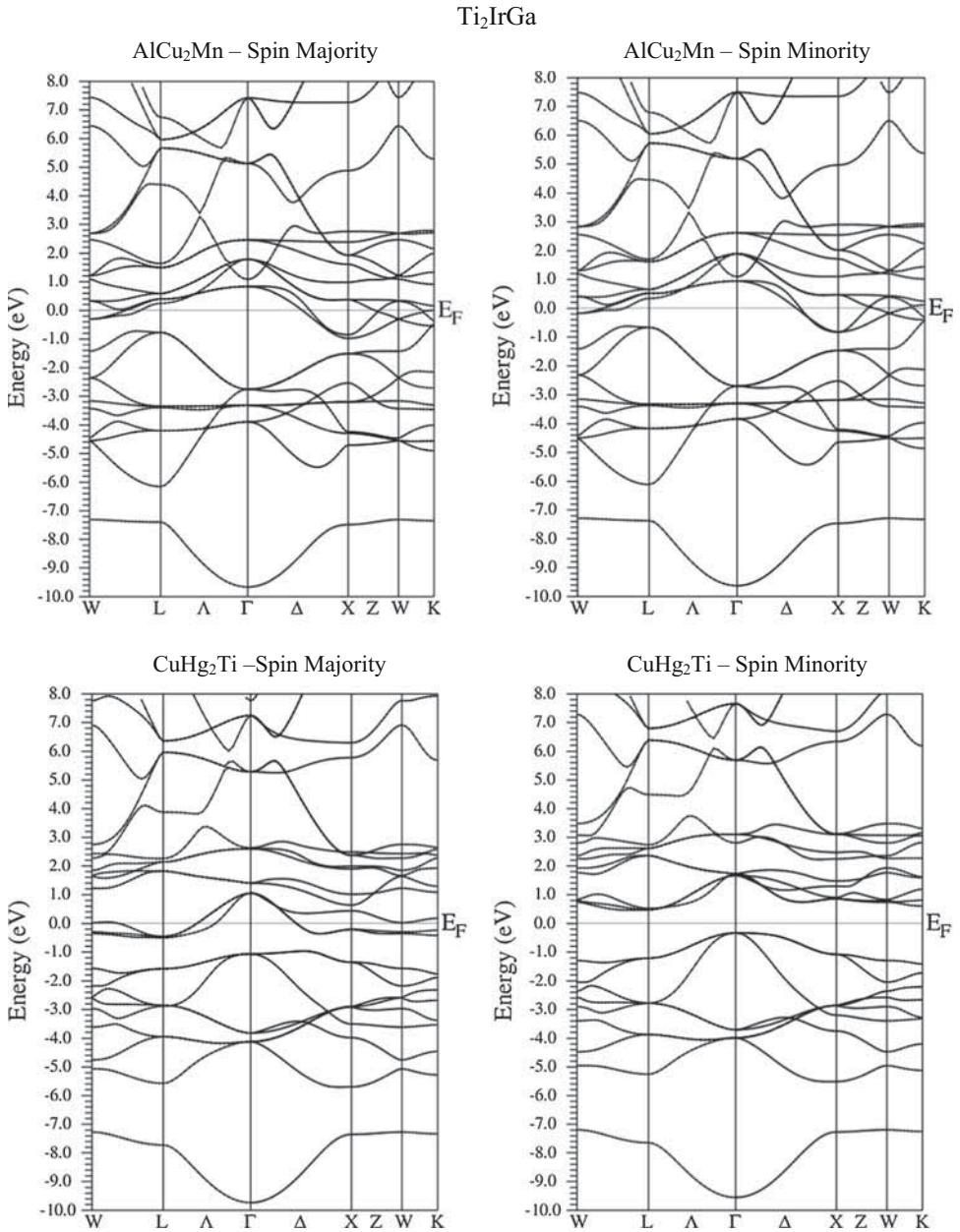

Figure 2. The band structures of Ti_2IrGa compound for $AlCu_2Mn$-type and $CuHg_2Ti$-type structures in majority and minority spin states at the equilibrium lattice parameter. The solid line at 0 eV indicates the Fermi energy (E_F).

to 6.5 eV are relative to antibonding states ($2 \times e_g^*$ and $3 \times t_{2g}^*$). The minority band gap can be attributed to the splitting between the bonding $3t_{2g}$ and non-bonding $3t_u$ states. In majority spin channel, the splitting exchange effect makes the energy bands shift towards lower energies and non-bonding $3t_u$ states cross the Fermi level. Therefore, $d-d$ hybridisation between transition metals of Ti and Ir is an important factor in the appearance of half-metallicity in Ti_2IrZ (Z = B, Al, Ga, and In) Heusler compounds.

The values of minority spin band gap (E_g) and HM band gap (E_{HM}) for the four HM compounds using LDA and GGA are reported in table 2. E_g can be calculated by subtracting the conduction band minimum (CBM) and valence band maximum (VBM) in the minority spin state. E_{HM} is defined as the minimum of the two magnitudes of VBM and CBM in minority spin state. Accordingly, the values of E_g and E_{HM} with GGA are higher than those obtained with LDA indicating that GGA predicts electronic structure of all compounds more realistically. Also, there is a relationship between the Z elements and the width of minority band gaps where E_g decreases by increasing the lattice constant along B→Al→Ga→In. According to table 2,

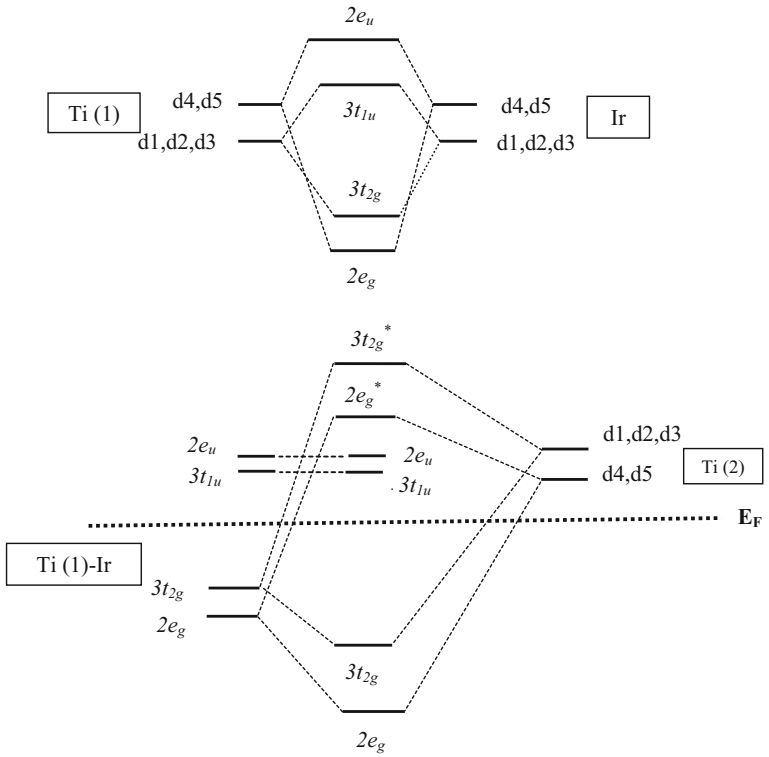

Figure 3. A schematic representation of the $d-d$ hybridisations between spin-down orbitals of Ti(1), Ti(2), and Ir transition metals at different sites for the Ti_2IrZ Heusler compounds.

Table 2. The minority spin (E_g) and half-metallic (E_{HM}) band gaps of Ti_2IrZ (Z = B, Al, Ga, and In) compounds at equilibrium lattice constants using LDA and GGA.

Compound	V_{XC}	E_g (eV)	E_{HM} (eV)
Ti_2IrB	GGA	0.87	0.27
	LDA	0.60	0.08
Ti_2IrGa	GGA	0.79	0.33
	LDA	0.54	0.11
Ti_2IrAl	GGA	0.75	0.28
	LDA	0.52	0.09
Ti_2IrIn	GGA	0.73	0.23
	LDA	0.53	0.05

it is concluded that with decreasing atomic number of Z element, VBM shifts to lower energies with respect to the Fermi level and minority band gaps increase. In fact, with decreasing atomic number of Z elements, the Coulomb repulsion decreases and minority band gaps increase [66].

Afterwards, the origin of half-metallicity and appearance of the minority band gap for Ti_2IrZ (Z = B, Al, Ga, and In) Heusler compounds in the $CuHg_2Ti$-type structure are investigated. For this purpose, the electronic density of states (DOSs) for Ti_2IrGa in the $CuHg_2Ti$-type structure as a representative of all compounds were also studied which are shown in figure 4. Accordingly, the existence of electronic states at the Fermi level in majority spin state and a band gap at the Fermi level in minority spin state confirm the HM characteristic of Ti_2IrGa compound. It is evident that there is a relatively strong hybridisation between the d states (t_{2g} and e_g) of transition metals Ti(1), Ti(2), and Ir around the Fermi level. As previously mentioned, this hybridisation makes d states split to three states: (1) bonding states below the Fermi level, (2) non-bonding states around the Fermi level, and (3) antibonding states above the Fermi level. Because of this hybridisation, the Fermi level is located in the gap between the bonding t_{2g} states and non-bonding t_u states. The $d-d$ hybridisation is the origin of the HM band gap in the full-Heusler alloys with $AlCu_2Mn$ structure [38]. Moreover, the bonding states below the Fermi level mainly belong to Ir with higher valence electrons, while the unoccupied antibonding states are mainly relative to Ti low-valent transition metal. This refers to the covalent hybridisation between high-valent and low-valent atoms which leads to the formation of minority spin band gap. The covalent hybridisation is mainly observed in half-Heusler compounds with $C1_b$ structure [38]. Therefore, half-metallicity originates from both covalent and $d-d$ hybridisations in Ti_2IrGa alloy. A similar behaviour is observed in other three compounds also.

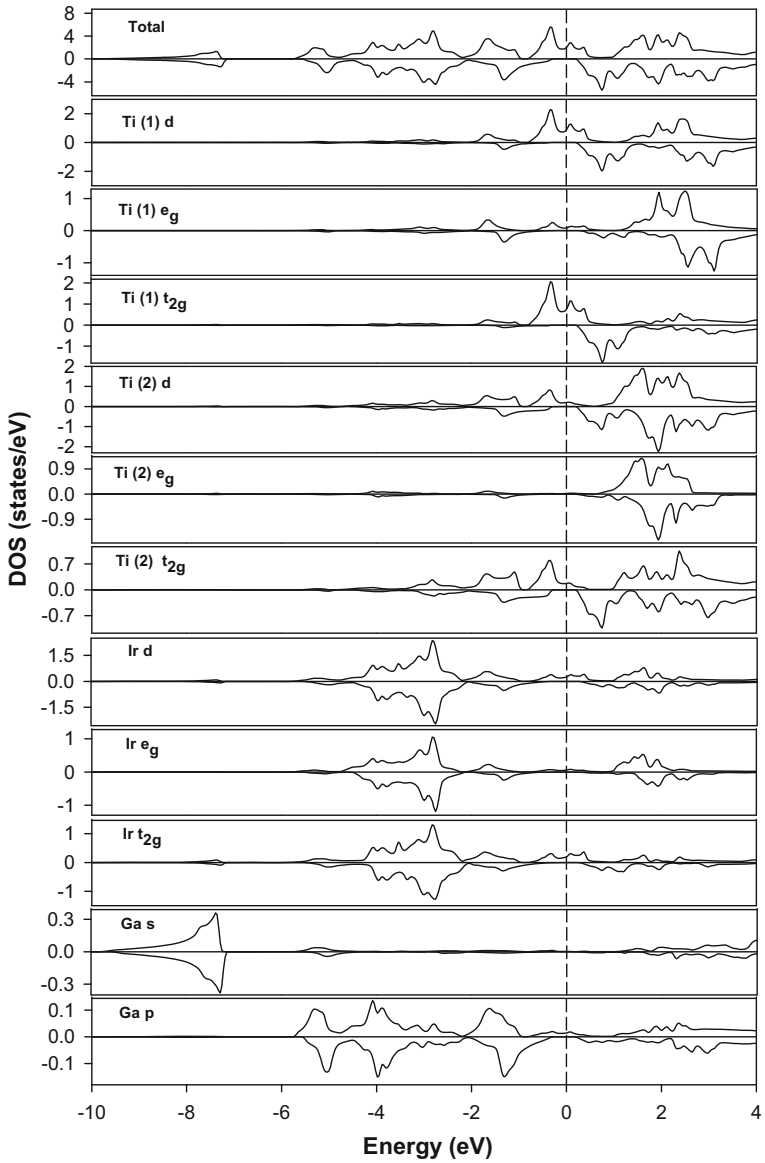

Figure 4. The total and partial DOSs for the Ti_2IrGa compound. Positive values of DOS are chosen as majority spin electrons and negative values as minority ones. The zero energy value corresponds to the Fermi level.

3.3 *The region of half-metallicity*

In order to investigate the sensitivity of half-metallicity with respect to change in lattice constant in detail, values of E_g at different lattice constants for Ti_2IrZ (Z = B, Al, Ga, and In) compounds in the $CuHg_2Ti$-type structure were calculated and plotted in figure 5. As can be seen, Ti_2IrB, Ti_2IrAl, Ti_2IrGa, and Ti_2IrIn compounds are half-metals between 5.61 and 6.73 Å, 5.63 and 6.80 Å, 5.51 and 6.80 Å, and 5.47 and 6.86 Å, respectively. By changing Z element along B→Al→Ga→In, the region of half-metallicity increases as 1.12 Å→1.17 Å→1.29 Å→1.39 Å, respectively. Among these compounds, Ti_2IrIn has the widest region of half-metallicity, showing its stability against negative and positive pressures. According to figure 5, there is a similar trend for Ti_2IrAl, Ti_2IrGa, and Ti_2IrIn compounds where VBM and CBM smoothly shift towards the Fermi level respectively by the expansion and compression of lattice and half-metallicity will be destroyed. For Ti_2IrB, by the expansion and compression of the lattice, CBM cuts the Fermi level and half-metallicity disappears.

3.4 *Magnetic properties*

The total and partial magnetic moments of Ti_2IrZ (Z = B, Al, Ga, and In) compounds in $CuHg_2Ti$-type structure using LDA and GGA are listed in table 3. Accordingly, the total magnetic moment (M_{tot}) for all the compounds

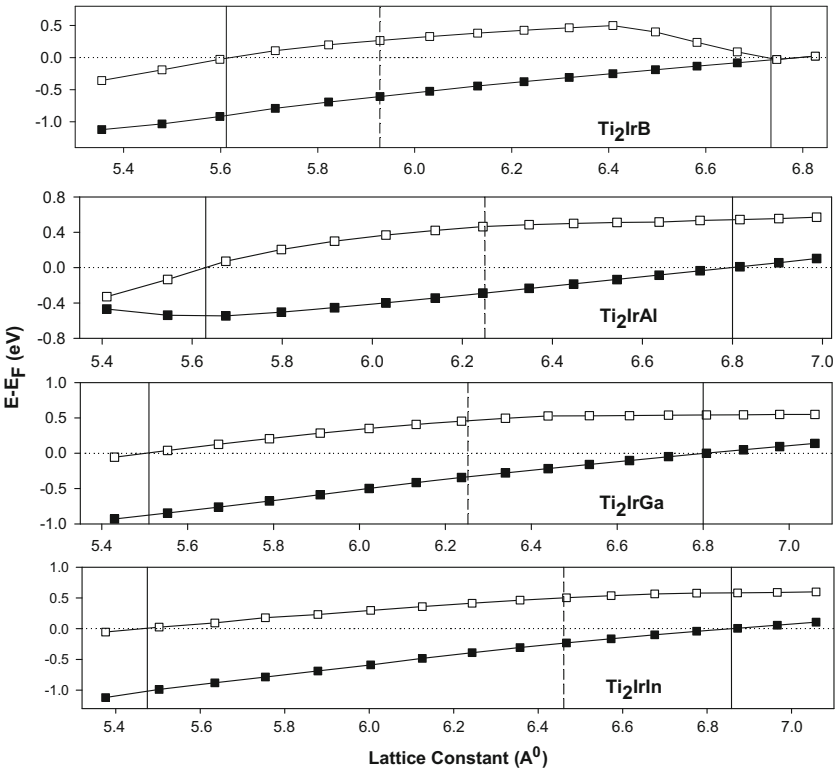

Figure 5. The minority band gap of Ti_2IrZ (Z = B, Al, Ga, and In) compounds in $CuHg_2Ti$-type structure as a function of the lattice constant. The black and white squares show the valence band minimum (VBM) and conduction band maximum (CBM), respectively. The vertical dashed line indicates the equilibrium lattice constant and vertical solid lines show the range of half-metallicity. The horizontal dotted line at 0 eV shows the Fermi energy.

Table 3. The total and atomic magnetic moments of Ti_2IrZ (Z = B, Al, Ga, and In) compounds using LDA and GGA. M_{tot} (μ_B): total magnetic moment; $M_{Ti(1)}$ (μ_B): Ti(1) magnetic moment; $M_{Ti(2)}$ (μ_B): Ti(2) magnetic moment; M_{Ir} (μ_B): Ir magnetic moment; M_Z (μ_B): Z magnetic moment; M_{Int} (μ_B): magnetic moment in the interstitial region.

Compound	V_{XC}	M_{tot}	$M_{Ti(1)}$	$M_{Ti(2)}$	M_{Ir}	M_Z	M_{Int}
Ti_2IrB	GGA	2.00	0.96	0.42	−0.008	−0.02	0.63
	LDA	1.95	0.95	0.41	−0.007	−0.01	0.57
Ti_2IrAl	GGA	2.00	0.98	0.38	−0.04	−0.0003	0.69
	LDA	1.93	0.95	0.34	−0.01	0.00	0.66
Ti_2IrGa	GGA	2.00	0.97	0.41	−0.04	−0.005	0.68
	LDA	1.91	0.91	0.40	−0.02	−0.001	0.60
Ti_2IrIn	GGA	2.00	0.96	0.42	−0.05	0.0005	0.67
	LDA	1.94	0.92	0.32	−0.03	0.00	0.60

using GGA are integer values of $2\mu_B$ while they are non-integer within LDA. M_{tot} in HM materials is usually an integer value. Therefore, GGA confirms that the four compounds are half-metals in $CuHg_2Ti$-type structure indicating that this approximation predicts the magnetic properties more appropriately. Furthermore, Ti_2IrZ (Z = B, Al, Ga, and In) compounds follow the generalised Slater–Pauling rule as $M_{tot} = Z_{tot} - 18$ in which Z_{tot} is the total number of valence electrons in the unit cell. Ti_2IrZ (Z = B, Al, Ga, and In) compounds have 20 valence electrons (4, 9, and 3 valence electrons for Ti, Ir, and Z, respectively). According to this rule, M_{tot} is obtained equal to $2\mu_B$ which is in a good agreement with the results of table 3 (by GGA).

Table 3 shows that the main contribution to M_{tot} comes from the Ti(1) and Ti(2) atoms. The magnetic moments of Ti(1) and Ti(2) atoms are not similar because the nearest neighbours of both atoms in $CuHg_2Ti$-type structure are different. The Ir atom has a small negative magnetisation. The Ir has nine valence

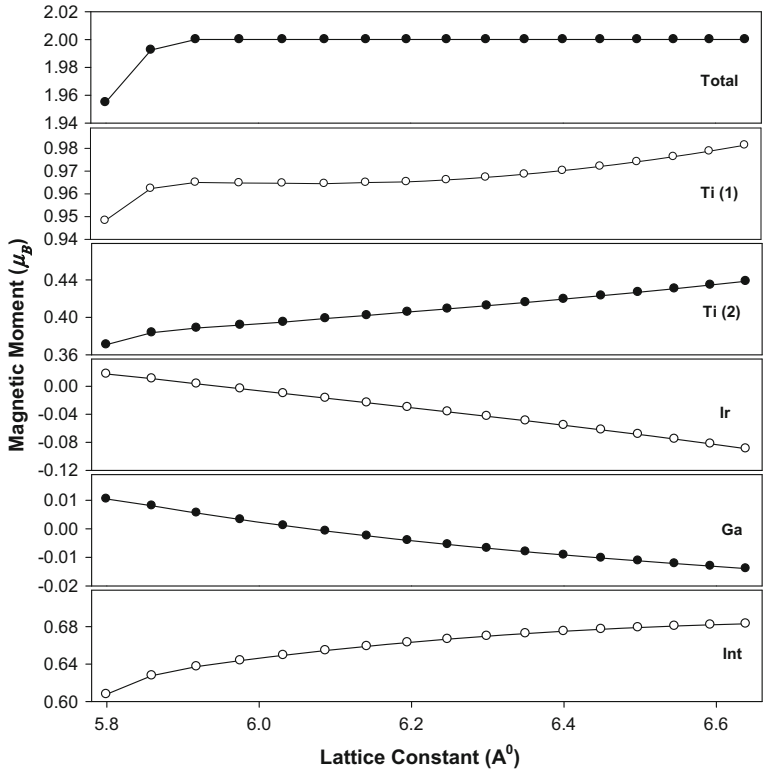

Figure 6. Total and atomic magnetic moments as functions of the lattice constant for Ti_2IrGa compound in $CuHg_2Ti$-type structure.

electrons and when hybridise with *d* electrons of Ti atoms, electrons tend to fill almost the complete *d* shell of Ir. Therefore, the magnetisation of Ti atoms increases and the magnetic moment of Ir decreases. The negative sign of the magnetic moment of Ir is due to a negative exchange splitting between spin-up and spin-down electrons in the *d* shell. The partial magnetic moment of Z elements are negligible which is due to the closed *p* shell arising from the $p-d$ hybridisation with transition metals. Similar results are observed in Zr_2CoZ and Zr_2CrZ (Z = Ga and In) compounds [67]. Furthermore, the contribution of interstitial region in magnetic moment is considerable in the four compounds. Since most of the *d* states exist in the muffin-tin spheres of the Ti(1), Ti(2), and Ir elements, the $d-d$ hybridisation mainly occurs inside muffin-tin spheres and magnetic moments in interstitial region enhances.

Finally, the magnetic properties of Ti_2IrZ (Z = B, Al, Ga, and In) compounds under compression and expansion deformations are investigated. For instance, M_{tot} and partial magnetic moments of Ti(1), Ti(2), Ir, Ga, and interstitial contribution as a function of lattice constant for Ti_2IrGa compound in the $CuHg_2Ti$-type structure are shown in figure 6. Accordingly, in a wide range of lattice parameters, $M_{tot} = 2\mu_B$ which shows that Ti_2IrGa has a HM nature within the wide range of lattice parameters. At high pressures, M_{tot} falls below the integer value of $2\mu_B$. With increasing lattice constant, the absolute magnetic moments of Ti(1) and Ti(2) increase. With increasing lattice constants, hybridisation between neighbouring atoms decreases and the behaviour of atoms tends toward isolated atoms which enhances their magnetisation. The magnetic moment of Ir and Ga atoms are positive at lower lattice constants while they are negative above 6 Å. This is due to the existence of the RKKY-type superexchange interaction between the *sp* elements and the transition metals which is recently mentioned by Hu and Zhang [68]. In fact, as this interaction is a long-range interaction, Ir and Ga atoms exhibit negative magnetic moments at high lattice constants.

4. Conclusion

The electronic structure and magnetism of Ti_2IrZ (Z = B, Al, Ga, and In) Heusler compounds were investigated using FP-LAPW method within DFT, within LDA and also within GGA for the exchange correlation potential. GGA predicts the electronic structure and magnetic properties of all compounds more appropriately. The calculations showed that the four compounds were half-metals in $CuHg_2Ti$-type structure. The origin

of half-metallicity was mainly relative to the $d-d$ and covalent hybridisations between transition metals Ti(1), Ti(2), and Ir. The range of half-metallicity for Ti_2IrB, Ti_2IrAl, Ti_2IrGa, and Ti_2IrIn compounds was 5.61–6.73 Å, 5.63–6.80 Å, 5.51–6.80 Å, and 5.47–6.86 Å, respectively. M_{tot} was an integer value of $2\mu_B$ for Ti_2IrZ (Z = B, Al, Ga, and In) Heusler compounds in the $CuHg_2Ti$-type structure which obeyed Slater–Puling rule of $M_{tot} = Z_{tot} - 18$. The negative magnetic moments of Ir and Ga atoms at high lattice constants were attributed to the RKKY-type superinteraction. Since the equilibrium lattice constants of the three Heusler compounds Ti_2IrZ (Z = Al, Ga, and In) in $CuHg_2Ti$-type structure were close to that of the semiconductors such as InSb (6.48 Å) and CdTe (6.49 Å) [69,70], it is suggested to grow these new HM alloys on suitable substrates to get new candidates for spintronic applications.

References

[1] S Chadov, T Graf, K Chadova, X Dai, F Casper, G H Fecher and C Felser, *Phys. Rev. Lett.* **107**, 047202 (2011)

[2] K Yakushi, K Saito, K Takanashi, Y K Takahashi and K Hondo, *Appl. Phys. Lett.* **88**, 082501 (2006)

[3] R A de Groot, F M Mueller, P G van Engen and K H J Buschow, *Phys. Rev. Lett.* **50**, 2024 (1983)

[4] Z H Zhu and X H Yan, *J. Appl. Phys.* **106**, 023713 (2009)

[5] K L Kobayashi, T Kimura, H Sawada, K Terakura and Y Tokura, *Nature* **395**, 677 (1998)

[6] A Nourmohammadi and M R Abolhasani, *Solid State Commun.* **150**, 1501 (2010)

[7] W Z Wang and X P Wei, *Comput. Mater. Sci.* **50**, 2253 (2011)

[8] J Dho, S Ki, A F Gubkin, J M S Park and E A Sherstobitov, *Solid State Commun*. **150**, 86 (2010)

[9] S Soeya, J Hayakawa, H Takahashi, K Ito, C Yamamoto, A Kida, H Asano and M Matsui, *Appl. Phys. Lett.* **80**, 823 (2002)

[10] L Kronik, M Jain and J R Chelikowsky, *Phys. Rev. B* **66**, 041203R (2002)

[11] N A Noor, S Ali and A Shaukat, *J. Phys. Chem. Solids* **72**, 836 (2011)

[12] I Galanakis and P Mavropoulos, *Phys. Rev. B* **67**, 104417 (2003)

[13] Y-Q Xu, B-G Liu and D G Pettifor, *Physica B* **329–333**, 1117 (2003)

[14] K L Yao, G Y Gao, Z L Liu and L Zhu, *Solid State Commun.* **133** , 301 (2005)

[15] K L Yao, G Y Gao, Z L Liu, L Zhu and Y L Li, *Physica B* **366**, 62 (2005)

[16] X-F Ge and Y-M Zhang, *J. Magn. Magn. Mater.* **321**, 198 (2009)

[17] F Ahmadian, *Pramana – J. Phys.* **77**, 383 (2011)

[18] S Datta and B Das, *Appl. Phys. Lett.* **56**, 665 (1990)

[19] K A Kilian and R H Victora, *J. Appl. Phys.* **87**, 7064 (2000)

[20] C T Tanaka, J Nowak and J S Moodera, *J. Appl. Phys.* **86**, 6239 (1999)

[21] J A Caballero, Y D Park, J R Childress, J Bass, W-C Chiang, A C Reilly, W P Pratt Jr and F Petroff, *J. Vac. Sci. Technol. A* **16**, 1801 (1998)

[22] C Hordequin, J P Nozieres and J Pierre, *J. Magn. Magn. Mater.* **183**, 225 (1998)

[23] P J Webster and K R A Ziebeck, *Alloys and compounds of d-elements with main group elements* (Springer, Berlin, 1988) Part 2, pp. 75, 184

[24] S Wurmehl, G H Fecher, H C Kandpal, V Ksenofontov, C Felser, H J Lin and J Morais, *Phys. Rev. B* **72**, 184434 (2005)

[25] I Galanakis, P Mavropoulos and P H Dederichs, *J. Phys. D: Appl. Phys.* **39**, 765 (2006)

[26] H C Kandpal, G H Fecher and C Felser, *J. Phys. D: Appl. Phys.* **40**, 1507 (2007)

[27] X-Q Chen, R Podloucky and P Rogl, *J. Appl. Phys.* **100**, 113901 (2006)

[28] K Özdoğan, I Galanakis, E Şasıoğlu and B Aktaş, *Solid State Commun.* **142**, 492 (2007)

[29] G D Liu, X F Dai, H Y Lui, J L Chen, Y X Li, G Xiao and G H Wu, *Phys. Rev. B* **77**, 14424 (2008)

[30] K Özdoğan and I Galanakis, *J. Magn. Magn. Mater.* **321**, L34 (2009)

[31] V Sharma, A K Solanki and A Kashyap, *J. Magn. Magn. Mater.* **322**, 2922 (2010)

[32] H Mori, Y Odahara, D Shigyo, T Yoshitake and E Miyoshi, *Thin Solid Films* **520**, 4979 (2012)

[33] G D Liu, X F Dai, H Y Liu, J L Chen and Y X Li, *Phys. Rev. B* **77**, 014424 (2008)

[34] H Z Luo, Z Z Zhu, L Ma, S F Xu, H Y Liu and G H Wu, *J. Phys. D: Appl. Phys.* **40**, 7121 (2007)

[35] I Galanakis, K Özdoğan, E Şasıoğlu and B Aktaş, *Phys. Rev. B* **75**, 172405 (2007)

[36] J Li, Y X Li, G X Zhou, Y B Sun and C Q Sun, *Appl. Phys. Lett.* **94**, 242502 (2009)

[37] N Xing, Y Gong, W Zhang, J Dong and H Li, *Comput. Mater. Sci*. **45**, 489 (2009)

[38] X-P Wei, J-B Deng, Ge-Y Mao, S-B Chu and X-R Hu, *Intermetallics* **29**, 86 (2012)

[39] F Ahmadian and R Alinajimi, *Comput. Mater. Sci.* **79**, 345 (2013)

[40] T Roy and A Chakrabarti, *Pramana – J. Phys.* **89**, 6 (2017)

[41] S Galehgirian and F Ahmadian, *Solid State Commun.* **202**, 52 (2015)

[42] H Y Jia, X F Dai, L Y Wang, R Liu, X T Wang, P P Li, Y T Cui and G D Liu, *J. Magn. Magn. Mater.* **367**, 33 (2014)

[43] L Wang and Y Jin, *J. Magn. Magn. Mater.* **385**, 55 (2015)

[44] M K Hussain, G Y Gao and K Yao, *J. Supercond. Novel Magn.* **28**, 3285 (2015)

[45] Q Fang, J Zhang and K Xu, *J. Magn. Magn. Mater.* **349**, 104 (2014)

[46] L Zhang, L Y Wang, J J Lu, X T Wang and L Wang, *J. Korean Phys. Soc.* **65**, 2058 (2015)
[47] M Liping, S Yongfan and H Yu, *J. Magn. Magn. Mater.* **369**, 205 (2014)
[48] N Kervan and S Kervan, *J. Phys. Chem. Solids* **72**, 1358 (2011)
[49] X Wei, G Mao, S Chu, H Deng, J Deng and X Hu, *J. Magn. Magn. Mater.* **341**, 122 (2013)
[50] F Ahmadian, *J. Korean Phys. Soc.* **64**, 277 (2014)
[51] A Birsan and P Palade, *Intermetallics* **36**, 86 (2013)
[52] H M Huang, S J Luo and K L Yao, *J. Magn. Magn. Mater.* **324**, 2560 (2012)
[53] E Bayar, N Kervan and S Kervan, *J. Magn. Magn. Mater.* **323**, 2945 (2011)
[54] S Kervan and N Kervan, *Solid State Commun.* **151**, 1162 (2011)
[55] Y Feng, B Wu, H Yuan, A Kuang and H Chen, *J. Alloys Compd.* **557**, 202 (2013)
[56] N Kervan and S Kervan, *J. Magn. Magn. Mater.* **324**, 645 (2012)
[57] A Birsan, P Palade and V Kuncser, *J. Magn. Magn. Mater.* **331**, 109 (2013)
[58] A Birsan, P Palade and V Kuncser, *Solid State Commun.* **152**, 2147 (2012)
[59] F Ahmadian, *J. Alloys Compd.* **576**, 279 (2013)
[60] F Taşkın, M Atiş, O Canko, S Kervan and N Kervan, *J. Magn. Magn. Mater.* **426**, 473 (2017)
[61] P Blaha, K Schwarz, G K H Madsen, D Hvasnicka and J Luitz, WIEN2k, an augmented plane wave local orbitals program for calculating crystal properties, Austria, Karlheinz Schwarz, Technische Universit Wien, ISBN 3-9501031-1-2; 2001
[62] J P Perdew and A Zunger, *Phys. Rev. B* **23**, 5048 (1981)
[63] J Perdew, K Burke and M Ernzerhof, *Phys. Rev. Lett.* **77**, 3865 (1996)
[64] F D Murnaghan, *Proc. Natl Acad. Sci. USA* **30**, 244 (1947)
[65] S Skaftouros, K Özdoğan, E Şasioğlu and I Galanakis, *Phys. Rev. B* **87**, 024420 (2013)
[66] K Özdoğan, I Galanakis, E Şaşioğlu and B Aktaş, *J. Phys.: Condens. Matter* **18**, 2905 (2006)
[67] Z Y Deng and J M Zhang, *J. Magn. Magn. Mater.* **397**, 120 (2016)
[68] Y Hu and J-M Zhang, *J. Magn. Magn. Mater.* **421**, 1 (2017)
[69] *Semiconductors: Physics of group IV elements and III–V compounds, Landolt–Börnstein, new series, group III* edited by O Madelung (Springer-Verlag, Berlin, 1982) Vol. 17, Pt. a
[70] *Semiconductors: Intrinsic properties of group IV elements and III–V, II–VI and I–VIII compounds, Landolt–Börnstein, new series, group III* edited by O Madelung (Springer-Verlag, Berlin, 1986) Vol. 22, Pt. a